

(1967).

²⁷G. J. Schulz, Phys. Rev. **112**, 150 (1958); **112**, 1141 (1959).

²⁸W. R. Henderson, W. L. Fite, and R. T. Brackmann, Phys. Rev. **183**, 157 (1969).

²⁹Calculations by Chapman and Herzenberg show that for an electron energy distribution 70 meV wide, the spikes in the rate constant are entirely resolved, while for a distribution slightly more than double this width, 150 meV, any structure is completely smeared out, producing an envelope similar to that obtained by Pack and Phelps. Further, according to these calculations, the

first peak of K_{\max} is reduced from 7.1×10^{-30} cm⁶/sec for 70-meV energy spread, to 3.9×10^{-30} cm⁶/sec for 150-meV energy spread, illustrating the sensitivity of the measured value on the incident electron energy spread.

³⁰The same apparatus has been used to measure the temperature dependence of other collision cross sections up to temperatures as high as 1300°K. However, in these cases the cross sections were larger and no signal averaging was required.

³¹G. J. Schulz (unpublished).

³²P. J. Chantry, J. Chem. Phys. **55**, 1851 (1971).

PHYSICAL REVIEW A

VOLUME 5, NUMBER 2

FEBRUARY 1972

Lifetimes, g Factors, and Collision Cross Sections of Hydrogen Molecules in the $(1s3p) \ ^3\Pi_u$ Level

M. A. Marechal, R. Jost, and M. Lombardi

Université Scientifique at Médicale de Grenoble, Laboratoire de Spectrométrie Physique, CEDEX-53, Grenoble-Gare 38, France

(Received 28 July 1971)

Experimental results obtained by Hanle and Bitter-Brossel effects on the $N=1$ and $N=2$ ($v=0, 1, 2$, and 3) levels of the $(1s3p) \ ^3\Pi_u$ state of the parahydrogen molecule excited by electron impact are presented. Resonances are found at the experimentally lowest possible frequencies (21–64 MHz) in a region where the $\underline{N} \cdot \underline{S}$ decoupling is nonexistent for the $N=2$ level [the measured Landé g factors are 0.77 ± 0.01 and 0.48 ± 0.02 corresponding to a pure Hund's-coupling case (b)] and just beginning for the $N=1$ level (at 21 MHz the apparent measured g is 1.235 ± 0.01). These results together with the calculations carried out in the case of complete $\underline{N} \cdot \underline{S}$ coupling lead to lifetimes $\tau = (3.10 \pm 0.3) \times 10^{-8}$ sec ($N=1$) and $\tau = (3.15 \pm 0.3) \times 10^{-8}$ sec ($N=2$) and $H_2^* - H_2$ cross sections $\sigma = 232 \pm 30 \text{ \AA}^2$ ($N=1$) and $\sigma = 240 \pm 30 \text{ \AA}^2$ ($N=2$). The quantities g , τ , and σ were all found to be independent on the vibrational number. Risk of cascade was eliminated.

I. INTRODUCTION

Recently, methods used in atomic spectroscopy have been successfully extended to molecular spectroscopy. They consist in studying excited states by level-crossing¹⁻⁹ (Hanle effect¹⁰) and magnetic resonance¹¹⁻¹⁴ (Bitter-Brossel effect¹⁵). Both of these effects are due to an alignment of an excited level (the Zeeman sublevels of different $|m|$ are inequally populated) created as described below by the excitation process. This alignment corresponds to a linear polarization of light emitted by this level (analogous effects exist in the case of circular polarization).

In the typical Hanle effect, one applies a static magnetic field at a right angle to the alignment direction (Fig. 1). In the classical explanation, the field produces a Larmor precession of the whole excited molecule, which, when averaged over the lifetime, gives a rotation of the plane of polarization and a partial depolarization of the emitted light. In the simple case where the fine and/or hyperfine coupling is not partially decoupled by the magnetic field (i. e., is either fully coupled, or fully decoupled), the width of the Hanle curve (per-

centage of polarization of the emitted light as a function of the magnetic field) gives the $g\tau$ product (g is the Landé g factor and τ the lifetime of the excited level).

In the typical Brossel effect, one applies a static magnetic field parallel to the alignment direction and a rf field perpendicular to the static field (Fig. 1). The polarization of the emitted light is determined by the difference of population of the Zeeman sublevels. When the frequency of the rf field is equal to the energy difference between the $\Delta m = 1$ Zeeman sublevels (single-quantum resonance), transitions are induced between those sublevels. The resulting modification of population of the sublevels gives a modification of the polarization of the emitted light. In the absence of intermediate coupling, the position of the Brossel resonance gives the value of g .

A knowledge of g and τ permits one to deduce the collision cross section σ from pressure broadening measurements of these curves and the coupling scheme of the angular moments. If magnetic resonance is carried out in the partial decoupling zone, fine or hyperfine structure can be determined.¹⁶

The first step in such an experiment is to excite

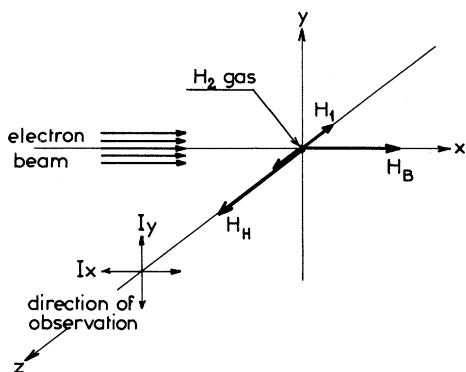


FIG. 1. Experimental set up. H_H represents the direction of the static magnetic field applied in the Hanle experiment; H_B and H_I are the static and rf fields applied in the Brossel experiment. I_x and I_y represent the intensities of the components of the light polarized along $0x$ and $0y$.

the molecule so as to align the excited level. This can be performed either by an optical or an electronic excitation. In the first experiments, the molecules were excited by nonisotropic light using, respectively, an atomic coincidence line (NO ,¹ OH ,⁵ and CS ⁷), a molecular resonance line (OH ,⁴ CO ,⁸ and CS ⁹), and a laser coincidence line (Na_2)⁶. The advantage of this method is that only a single or a small number of rotational levels are excited; the analysis of the emitted light is thus simplified. The disadvantage is that only a few molecular levels are accessible by this method and frequently they have high rotational quantum numbers. Moreover, until now only excited levels which are optically connected with the ground state have been studied.

These restrictions disappear when the molecules are excited by electron impact. In this case all excited levels can be populated. During the electron-molecule collision part of the kinetic energy of the electron is transferred to the molecule and, when the electronic beam has a well-defined direction, the excited molecular level is aligned. A simple explanation of these phenomena and their relation with the conservation of angular momenta is given by Lamb.¹⁶ This procedure, which is an extension to molecules of the experiment performed by Skinner and Appleyard¹⁷ on atoms, was carried out on the H_2 molecule by Cahill, Schwartz, and Jette.¹⁸ The excitation can be obtained with a continuous electron beam in a triode glass cell,¹⁹ or with a high-frequency discharge.²⁰ Nevertheless, some difficulties are inherent to this method: (i) weak emission of the excited molecular level j_j ; (ii) emission from all excited levels; the separation of the line emitted by different rotational levels necessitates a monochromator of high resolution;

this separation is easier for molecules with low moment of inertia such as H_2 ; (iii) risk of cascades; the excited level being examined can be populated by de-excitation of an upper level; in this case, the experimental results concerning the level studied are strongly perturbed; and (iv) limitation of the static magnetic field strength which can perturb the electron beam. The electronic excitation has been used until now only to excite the H_2 molecule. Van der Linde and Dalby have performed a Hanle experiment³ on H_2 excited by a high-frequency discharge; simultaneous experiments in our laboratory were performed on the Hanle effect² and Brossel effect¹¹ in H_2 excited in a triode glass cell.

We present here the results of the Hanle experiment and Brossel experiment concerning different rotational and vibrational levels of the $(1s3p) \ ^3\Pi_u$ electronic state of the H_2 molecule. In Sec. II, we establish the algebraic form of the Hanle curve and the Brossel curve when the fine structure is not optically resolved. In Sec. III, we describe the experimental setup and the results. In Sec. IV, we discuss the experimental results: the variation of the g factor with the magnetic field (and the frequency) which shows the beginning of a $\underline{N} \cdot \underline{S}$ decoupling; the extrapolated, measured g value which permits us to deduce the type of Hund's coupling; and the lifetime τ and the collision cross section ($\text{H}_2^* - \text{H}_2$) σ . In Sec. V, we discuss the validity of those results, and show that the effect of cascading is negligible in our results.

In this paper, we are limiting ourselves to Brossel experiments realized at the lowest possible frequency (i. e., 21 and 35 MHz) imposed by the width of the resonance curves, i. e., by the $g\tau$ product for the studied level. We shall see that this fact limits us to the region where the $\underline{N} \cdot \underline{S}$ decoupling is only beginning for the $N=1$ levels, and is nonexistent for the $N=2$ levels. Due to this fact, the calculations carried out in Sec. II are based on a complete $\underline{N} \cdot \underline{S}$ coupling scheme. Further experiments performed in the $\underline{N} \cdot \underline{S}$ decoupling zone and concerning the $N=1$ levels will be described and interpreted in Paper II.²¹

II. ALGEBRAIC EXPRESSION OF HANLE AND BITTER-BROSSEL CURVES

In the case of diatomic molecular levels, the Landé g factors are determined by the coupling scheme of the different angular momenta (Hund's case)²²: the projection Λ of the electronic orbital angular momentum \underline{L} along the intermolecular axis, the pure rotational angular momentum \underline{O} , and the electronic spin \underline{S} . Hydrogen is either a "b" or a "d" Hund's case or an intermediate case. In either case, the sum of the electronic and rotational angular momenta, \underline{N} , is a constant of the motion.

\underline{S} and \underline{N} will couple to give the total angular momentum $\underline{J} = \underline{S} + \underline{N}$. In a triplet state ($S=1$), this interaction splits a given rotational level \underline{N} into three levels characterized by J ($J=N, N\pm 1$). The energy splitting gives the fine structure. We suppose, in this section, that the fine structure is sufficiently large that the Hanle and Brossel magnetic fields do not perturb the $\underline{N}\cdot\underline{S}$ coupling. Thus, J is a good quantum number. We will discuss the validity of this hypothesis in Sec. IV. Each of these levels is characterized by a corresponding g_J factor, and they have the same lifetime τ_N . The transitions originating in these three levels are not optically separated. Hence in the Hanle and Brossel experiments, we observe three contributions due to each fine structure level. We wish to establish the way in which these contributions combine in each experiment.

Figure 1 shows the direction of the electronic beam, of the observation, and of the respective magnetic fields (H_H and H_B are the static fields applied in the Hanle and the Brossel experiments, H_1 is the rf field). The hydrogen gas sample is placed at the origin. The quantity we measure experimentally is the polarization ratio P ;

$$P = (I_x - I_y)/(I_x + I_y). \quad (1)$$

We shall now calculate the variation of P with the static magnetic field. The following calculation is a direct application of the theoretical work of D'Yakonov²³ and Nédélec.²⁴ It could equally well be carried out using the formalism of Percival and Seaton.²⁵

A. Hanle Effect

The observed intensity $I(\vec{u}, \lambda)$ derived from the D'Yakonov theory and expressed in the notation of Omont and Meunier²⁶ is

$$I(\vec{u}, \lambda) = I_0 \sum_{J'k} B_k (JJ'NN_0S) \sum_q^{JJ'} \rho_q^k \phi_q^k(\vec{e}_{\vec{u}, \lambda}),$$

where

$$B_k = (-)^{2N_0 + N + S + k + J'} \left| (2k+1)(2J+1)(2J'+1) \right|^{1/2} \\ \times \begin{Bmatrix} 1 & 1 & k \\ N_0 & N_0 & N \end{Bmatrix} \begin{Bmatrix} J & J' & k \\ N_0 & N_0 & S \end{Bmatrix}.$$

The components $^{JJ'}\rho_q^k$ are the density matrix components on the tensorial operator basis $^{JJ'}\underline{T}_q^k$ defined by Omont.²⁶ These operators are defined in the laboratory frame. We have no need in this work to express them in the molecular frame. $\phi_q^k(\vec{e}_{\vec{u}, \lambda})$ are known functions determined by the direction of polarization used to analyze the emitted light.²³ N and N_0 are the initial and final rotational states of the optical transition. If we assume that the fine structure A is much greater than both $1/\tau$ and ΔE , the Zeeman splitting (i. e., no $\underline{N}\cdot\underline{S}$ de-

coupling), the stationary solution of the density matrix equation is

$$^{JJ'}\rho_q^k = \frac{^{JJ'}\rho_q^{(0)k}}{\Gamma - i q g_J \mu_B H} \quad (2)$$

for the diagonal terms in J . The nondiagonal terms which are smaller by a factor Γ/A are neglected. In (2), $\rho^{(0)}$ is the electronic excitation density matrix referred to a quantization axis defined by the static magnetic field (in the Hanle experiment, this direction is $0z$). The molecular excitation is produced by an electron-molecule collision. Using the hypothesis of Percival and Seaton,²⁵ we assume there is an equal probability for populating all of the spin states. It follows that the excitation matrix $\rho^{(0)}$ of the level N is the direct product of an isotropic (i. e., unity) density matrix in spin space \underline{U} and an anisotropic density matrix in N space. This excitation matrix can also be expressed in the tensorial coupled basis:

$$\rho^{(0)} = \sum_{kq} N \rho_q^{(0)k} \frac{\underline{U}}{2S+1} \times N \underline{T}_q^k \\ = \sum_{JJ'} \sum_{kq} ^{JJ'}\rho_q^{(0)k} ^{JJ'}\underline{T}_q^k. \quad (3)$$

The $^N\underline{T}_q^k$ operators as defined by Omont²⁶ operate in the N space alone. The solution of (3) gives

$$^{JJ'}\rho_q^{(0)k} = N \rho_q^{(0)k} \cdot C_{JJ'}^k,$$

with the $C_{JJ'}^k$ being given by the following expression (Messiah²⁷):

$$\langle J || \frac{\underline{U}}{2S+1} \times N \underline{T}^k || J \rangle = C_{JJ'}^k \langle J || ^{JJ'}\underline{T}^k || J \rangle,$$

i. e.,

$$C_{JJ'}^k = \frac{1}{(2k+1)^{1/2}} (-)^{J+N+S+k} \frac{2J+1}{2S+1} \begin{Bmatrix} N & k & N \\ J & S & J \end{Bmatrix}.$$

The excitation density matrix $^N\underline{\rho}^{(0)}$ expressed in the static magnetic field quantization axis is obtained from the excitation density matrix $^N\underline{\rho}^{(00)}$ expressed in the electron beam quantization axis by a rotation R through $\frac{1}{2}\Pi$ around the $0y$ axis. Because of the electron beam axial symmetry, the decomposition of $^N\underline{\rho}^{(00)}$ in a tensorial operator basis,

$$^N\underline{\rho}^{(00)} = \sum_{kq} N \rho_q^{(00)k} N \underline{T}_q^k,$$

gives only terms even in k . Moreover, because the observed transition is of electric dipole character, only the $k=0$ and $k=2$ terms occur in the Hanle and Brossel experiment.^{23,24} Those of higher order will occur in a nonzero field level crossing experiment (Descoubes²⁸). Thus we have

$$\times \left| \frac{1}{4} \sqrt{6} \ N \underline{T}_2^2 - \frac{1}{2} \ N \underline{T}_0^2 + \frac{1}{4} \sqrt{6} \ N \underline{T}_{-2}^2 \right|.$$

So (1) becomes

$$P = P_0 \sum_J B_2 C_{JJ}^2 \frac{1}{\Gamma^2 + (g_J \mu_B H)^2} = P_0 \sum_J h_J Y(J, H).$$

Thus the Hanle effect gives three superimposed Lorentzians $Y(J, H)$ of relative height

$$h_J = (2J+1)^2 \left\{ \begin{matrix} N & 2 & N \\ J & S & J \end{matrix} \right\}^2 \quad (4)$$

and full width at half-height

$$H_J = \frac{1.137 \times 10^{-7}}{g_J \tau_N} \text{ Oe} \quad (5)$$

B. Brossel Effect

An analogous argument is used, but with quantization axis Ox (direction of static field and electron beam), the observation still being made along the Oz axis. We shall calculate the quantity

$$P' = \frac{I_x - I_y}{I_x + 2I_y} = \frac{2P}{3 - P}, \quad (6)$$

which can be considered to be proportional to P in the present case provided P is less than 10%. The solution of the density matrix equation gives a time-independent term which is a function of $H^{23,24}$:

$$\begin{aligned} {}^J J \rho_0^2 &= \frac{1}{\Gamma} \quad {}^J J \rho^{(00)2} \\ &\times \left| 1 - \frac{3\Omega_J^2 (4\delta_J^2 + \Omega_J^2 + \Gamma^2)}{(\delta_J^2 + \Gamma^2 + \Omega_J^2) (4\delta_J^2 + \Gamma^2 + 4\Omega_J^2)} \right| \\ &= \frac{{}^J \rho^{(00)2}}{\Gamma} [1 - R(J, H)], \end{aligned} \quad (7)$$

with

$$\Omega_J = g_J \mu_B H_1, \quad \delta_J = (\omega - g_J \mu_B H), \quad \text{and} \quad \Gamma = 1/\tau,$$

where $R(J, H)$ is the traditional double-resonance curve.¹⁵ Making use of expression (7), (6) becomes

$$P' = P_0' \left| 1 - \sum_J (2J+1)^2 \left\{ \begin{matrix} N & 2 & N \\ J & S & J \end{matrix} \right\}^2 R(J, H) \right|.$$

The Brossel effect thus gives three separate resonances centered at

$$H_J = \frac{\omega}{g_J \mu_B}$$

and of relative height

$$h_J = (2J+1)^2 \left\{ \begin{matrix} N & 2 & N \\ J & S & J \end{matrix} \right\}^2 \frac{b_J^2}{1 + 4b_J^2},$$

where

$$b_J = \frac{g_J \mu_B H_1}{\Gamma}. \quad (8)$$

It can be seen that the relative heights of the three resonances depend on the strength of the rf field H_1 : in the limit as $b \rightarrow 0$,

$$h_J \sim (2J+1)^2 \left\{ \begin{matrix} N & 2 & N \\ J & S & J \end{matrix} \right\}^2 g_J^2;$$

in the opposite limit, as $b \gg 1$,

$$h_J \sim (2J+1)^2 \left\{ \begin{matrix} N & 2 & N \\ J & S & J \end{matrix} \right\}^2.$$

III. EXPERIMENTAL

The molecular excitation is induced by an electronic beam directed along the Ox axis (Fig. 1) in a triode glass cell¹⁹ which contains gaseous hydrogen. This cell is connected to a pumping system which controls the pressure. The pressure, measured with a Mediovac gauge which is calibrated against a McLeod gauge, is measured with a precision of about 10%. The electrons are accelerated through 30 V which was found to be the optimum value. The anode-cathode current is of the order of 10 mA. The cathode is heated by a current of 1.2 A; this current is ac in the Brossel experiment in order to eliminate any shift of the center of the resonance line due to any stray dc magnetic field (the resulting broadening of the resonance is negligible). A thermoprobe placed at different spots between the grid and the plate indicates a temperature of about 800 °K. A Doppler linewidth measurement on the 6224-Å molecular line places an upper limit of a 1000 °K on the gas temperature.

The light emitted along the Oz axis (Fig. 1) is analyzed using a Jobin-Yvon-type HRS 1 monochromator with a slitwidth assuring a resolution between 2 and 5 Å during the experiment, and is detected by an EMI 9558 QB photomultiplier cooled to -50 °C. The polarization ratio P , given by Eq. (1), of the selected line is measured by a rotating Polaroid system.²⁰ This quantity is then recorded as a function of the magnetic field either on a X-Y recorder for the Hanle experiment or is accumulated in a multichannel (100 channels) over 10-30 h in the Brossel experiment.

The static magnetic fields (see Fig. 1 and Sec. II) are known with a precision of 10^{-3} . The stability of the frequency of the rf field H_1 (Fig. 1) is 1 part in 10^5 .

IV. EXPERIMENTAL RESULTS AND THEIR INTERPRETATIONS

We examine the electronic transition $(1s\ 3p)^3\Pi_u - (1s\ 2s)^3\Sigma_g^-$. In particular, we study the two lowest rotational levels $N=1$ and $N=2$ within the four lowest vibrational levels $v=0, 1, 2$, and 3 of the electronic state $(1s\ 3p)^3\Pi_u$. In order to avoid complications due to the hyperfine structure, we select

the transition coming from parahydrogen (nuclear spin $I=0$), which are the $N=1 \rightarrow N_0=0$ (R branch) and $N=1 \rightarrow N_0=2$ (P branch) for $N=1$ and $N=2 \rightarrow N_0=2$ (Q branch) for $N=2$. For $N=1$, we choose the R branch because it is much more polarized.

A. Preliminary Discussion

We notice at first that the experimental measurements are independent of the vibrational level in the limit of the experimental precision. Before interpreting these measurements we must be sure that the Hanle and the Brossel curves are attributable to the upper level of the examined transition and not to another higher level observed by cascade. We shall check this assumption in Sec. V.

Furthermore, in order to know the g value at zero magnetic field we have to know if the applied magnetic field is strong enough to partially or totally decouple \underline{N} and \underline{S} . This happens if the Zeeman energy separation is not negligible compared to the fine structure, which at this stage is unknown. We can nevertheless roughly evaluate it by an extension of the theoretical work of Chiu²⁹: The smallest value of this fine structure is obtained for the separation of the $J=1$ and $J=2$ fine levels of the $N=1$ rotational levels. For these levels, assuming a pure Hund's-coupling case (b)³⁰ and in the case of a total $\underline{N} \cdot \underline{S}$ coupling (case I) the theoretical g values³⁰ (Table II) imply that the $J=1$ and $J=2$ components collapse into one curve with a g factor of 1.251; the $J=0$ component is isotropic and cannot show any polarization-dependent effect (case I is always realized in the Hanle effect assuming that the fine structure A is much greater than $1/\tau$). In the case of total $\underline{N} \cdot \underline{S}$ decoupling (case II) only a $N=1$ component occurs with a g factor equal to 0.5. In the Brossel experiment, with increasing magnetic field (i. e., going from case I to II) we expect the following evolution: The single resonance becomes broad and separates in six resonances; at very high field, three of them become pure spin resonances ($\Delta |m_s| = 1$) with $g=2$, whose amplitudes go to zero, while three other resonances become pure orbital resonances ($\Delta |m_N| = 1$) with $g=0.5$.

In the $N=2$ case, the theoretical fine structure is large enough, and no $\underline{N} \cdot \underline{S}$ decoupling is expected to occur in our experiment. On this level there are three curves, $J=1, 2$, and 3 , with the theoretical g factors 0.473, 0.751, and 0.779, respectively (Table II), assuming a pure Hund's-coupling case (b).

Zero-Pressure Linewidth

In the Brossel experiment, the pressure was sufficiently low ($\sim 5 \cdot 10^{-3}$ Torr) so as not to perturb the linewidth. This implies that, in the case when the broadening due to $\underline{N} \cdot \underline{S}$ decoupling can be neglected, the line broadening observed is due only to the strength of the rf field H_1 .

In a level without fine structure (only one Brossel or Hanle component), the full width at half-maximum (FWHM) ΔH_B of the Brossel resonance line tends to $2\Delta H^0$ (ΔH^0 being the extrapolated zero-pressure Hanle FWHM) as H_1 tends to zero.¹⁵ Then, for a given strength H_1 the ratio of this compared to $2\Delta H^0$ gives the parameter $b = g \mu_B H_1 \tau$. In our case, when the fine structure separates each of the two effects in three curves characterized by J and g_J (which we shall call the J components), the parameter $b_J = g_J \mu_B H_1 \tau$ can be defined as above (Sec. II). This parameter is then determined as follows.

For the $N=1$ level we have seen that at low magnetic field the three J components collapse into one. Hence, the b value ($b_1 = b_2$) is directly known by comparing the width of the Hanle and Brossel curves.

For the $N=2$ level using the above values of the g factor the Hanle effect is composed of three Lorentzians of relative FWHM, $\Delta H_1^0 = \Delta H_3^0 = \frac{2}{3} \Delta H_2^0$, and relative heights given by (4); $h_2/(h_1 + h_3) = \frac{1}{4}$. This permits us to calculate the absolute value of ΔH_J^0 from ΔH^0 , the zero-pressure extrapolated FWHM of the Hanle curve (Table I). The b_J parameter is measured here by comparing the FWHM of the Brossel J component, with the previously deduced ΔH_J^0 value of the corresponding Hanle J component.

Pressure Effects

The g factor extrapolated at zero field permits us to deduce the lifetime τ_N from Hanle width extrapolated at zero pressure using expression (5) (Table II). The $H_2^* - H_2$ collision cross section σ is obtained from the slope of the function $\Delta H = f$ (pressure) (Fig. 2) using the Mitchell and Zemansky expression³¹

$$\sigma = \frac{1}{\tau P} \left(\frac{\pi k T m}{8} \right)^{1/2} \quad (9)$$

B. Results

Hanle Results

We found a Hanle effect¹⁰ (i. e., depolarization as function of magnetic field) for the above mentioned transitions. In Fig. 2, we plot the FWHM ΔH of the depolarization curves as a function of pressure. By extrapolation we deduce ΔH^0 , the value of ΔH at zero pressure (Table I).

Brossel Results

We have also performed a magnetic resonance¹⁵ experiment (i. e., Brossel effect) for the same transitions. In Table I, we present the apparent g factors deduced from the positions of the resonances the real g values being by definition the extrapolated zero-frequency g factors (these values are the result of a large number of measurements carried out at different H_1 strengths).

TABLE I. Zero-pressure extrapolated FWHM ΔH^0 of the Hanle curve and apparent experimental g values. The ΔH_J^0 value of the Hanle component is calculated from ΔH^0 . The b_J parameter is obtained by comparison of the FWHM ΔH_B of the Brossel resonance line with ΔH_J^0 .

Vibrational $v \rightarrow v_0 = v$	Rotational $N \rightarrow N_0$	λ (Å)	ΔH^0 (Oer) Hanle expt.	$\omega/2\pi$ (MHz)	Apparent g value	ΔH_B^a (Oe) Brossel expt.	b^a parameter	Height ^a of Brossel curve (a.u.)		
0	1 → 0	5994	3.1 ± 0.3	21	1.235 ± 0.01	8.15 ± 0.15	~0.4			
				35	1.215 ± 0.01					
				64	1.18 ± 0.02					
1	...	6098	3.1 ± 0.3	35	1.215 ± 0.015	12.5 ± 0.5	no sense			
2	...	6201		35	1.21 ± 0.02					
3	...	6303		35	1.215 ± 0.02					
0	2 → 2	6023	5.1 ± 0.5	21	0.77 ± 0.01	10.2 ± 0.5	~0.1			
1	...	6127		35	0.78 ± 0.02				10 ± 0.5	~0.1
				35	0.78 ± 0.02				13 ± 0.5	~0.4
2	...	6230	35	0.51 ± 0.04	15 ± 0.5	~0.5	20 ± 1			
				0.77 ± 0.01			21 ± 2	3.5 ± 1		
					0.48 ± 0.01					

^aEach result in these columns concerns one particular experiment performed at a given H_1 value; comments are given in Sec. IV.

We present also the measured FWHM, relative height, and b parameter for particular experiments.

$$N = 1$$

The observed results need some comments

Figure 3 shows a resonance obtained at 21 MHz on the 5994-Å line with comparatively high H_1 value. The b value ($b \sim 0.4$) obtained in this manner as well as the typical line shape indicates that we are close to the Brossel reversal condition; then, comparing the relative heights of this resonance to the Hanle curve relative to this line, we find a ratio of $\frac{1}{3}$. This last measurement will be used to disprove the existence of one kind of cascading (Sec. V).

At 35 MHz the resonance curve is slightly broadened even at very low rf field.

At 64 MHz the resonance, realized at very low rf field, shows an important broadening (FWHM of 12.5 ± 0.5 Oe); the center of gravity corresponds to an apparent g factor of 1.18 ± 0.02 , and the shape of the curve is asymmetric.

The experimental results at 21, 35, and 64 MHz, on the 5994-Å line ($N=1$ level) show that the resonances occur at the beginning of the $N \cdot S$ decoupling [resonance at lower magnetic field could not be performed because of the width of the resonance curve implying an overlap with the symmetrical resonance at $-\omega$ (see Fig. 3)]. The difference between the measured g factors at 64 MHz (1.18), 35 MHz (1.215), and 21 MHz (1.235) is greater than the experimental precision.

A study of this decoupling is described in Paper II,²¹ by performing resonances at higher frequency and giving the value of the fine structure. Then, the Zeeman diagram shows that the g factors deduced from the resonances centered at 20.5 Oe (35 MHz) and 12.5 Oe (21 MHz) must be corrected by +0.035 and 0.013, respectively, in order to obtain the g value at zero magnetic field. This value was found to be 1.249 ± 0.10 .

$$N = 2$$

The Brossel results (Table I), concerning the

TABLE II. Theoretical and experimental g values. Lifetime τ_N is deduced from the Hanle width extrapolated at zero pressure using the zero-field extrapolated g factor and Eq. (5). Collision cross section σ is obtained from the slope of pressure curve (Fig. 2) and Eq. (9).

Vibrational $v \rightarrow v_0 = v$	Rotational $N \rightarrow N_0$	J	g^a theor.	g expt. extrapolated	τ_N (sec) expt.	σ_N (Å ²) expt.
$v=0, 1, 2, 3$	1 → 0	0	1.251	1.249 ± 0.010	$(3.10 \pm 0.3) \times 10^{-8}$	(232 ± 30)
		1				
		2				
-0, 1, 2, 3	2 → 2	2	0.473	0.48 ± 0.02	$(3.15 \pm 0.3) \times 10^{-3}$	(240 ± 30)
		1	0.751	0.77 ± 0.01		
		3	0.778			

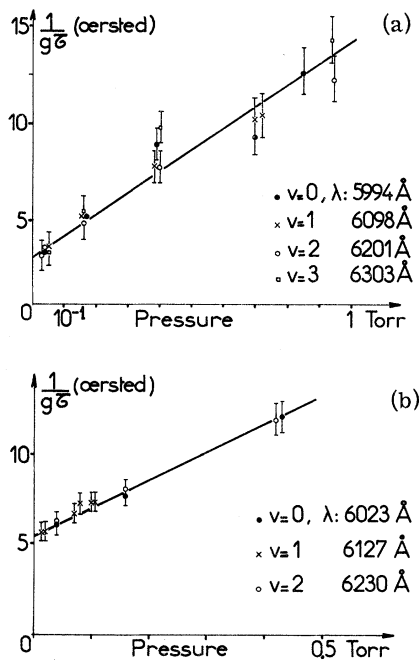


FIG. 2. Pressure broadening on the Hanle effect. The full width at half-height $1/g\tau$ of the Hanle curve is plotted as a function of the pressure. The Hanle effect is observed successively on (a) a R_0 ($N=1 \rightarrow N_0=0$), and (b) a Q_2 branch ($N=2 \rightarrow N_0=2$) of the electronic transition ($3p^3\Pi_u \rightarrow ^3\Sigma_g$) for different vibrational levels v .

$N=2$ level, require two comments. The $J=2$ resonance component has been detected with a g value of 0.48, coinciding with the expected one (Table II). The $J=1$ and $J=3$ resonance components have not been separated; the measured mean g value of this group of resonances, $g=0.77$, can be understood if we compare the calculated height (4) of the $J=1$ ($h_1=21$) and the $J=3$ ($h_3=96$) components with the corresponding calculated $g_1=0.751$ and $g_3=0.779$. At low H_1 ($b_1 \lesssim 0.1$) we only detect the resonance group resulting from the $J=1$ and 3 levels, whereas at high H_1 ($b_1=0.5$) the $J=2$ resonance appears together with the $J=1$ and 3 resonance group.

These experimental results, may be understood if we use the expression (8) which gives the relative height of the 2 resonance groups

$$\frac{h_2}{h_1+h_3} = \frac{1}{9} \frac{1+4b_1^2}{1+1.8b_1^2}.$$

This ratio varies from $\frac{1}{9}$ ($b_1 \lesssim 0.1$) to $\frac{1}{4}$ ($b_1 \gg 1$). In the first case, the $J=2$ resonance is not detectable because of the bad signal-to-noise ratio. When $b_1=0.5$, the calculated ratio is $\frac{1}{6}$, which is in agreement with the experimental result (Table I).

For the $N=2$ levels, we can conclude that the resonance at 21 and 35 MHz occur out of the decoupling region and that the measured g factors can be

considered as zero-field g values.

The agreement between the measured and calculated g factors (Table II) allows us to conclude that for these two levels (within the experimental resolution) we have a pure Hund's case (b).

The zero-field g factors determined in the above manner permit us to deduce τ_N and σ_N from the Hanle results for the considered levels (Table II). This cross section is an intrinsic constant of the studied level in the case where this level is not populated by transfer³² during the collision.

V. DISCUSSION

The preceding results are attributable to the $(1s3p)^3\Pi_u$ electronic state in the limit where no cascades occur [i. e., the $(1s3p)^3\Pi_u$ state being studied, which we will call level A, is not populated by de-excitation from upper levels (B levels)]. In order to eliminate this possibility we shall briefly recall how a cascade modifies the Hanle and the Brossel curves.^{24,33}

When a cascade occurs, the Brossel effect due to level A can be, in general, separated from that due to B, because of the difference in Landé g factor (except the improbable case of an accidental equality of g); but the Hanle effect is the combination of two depolarization effects coming from each level.

If the upper level (cascading level) has a value of $g\tau$ much larger than that of the level A, the Hanle effect can be considered as the sum of two depolarization curves: a narrow one coming from the upper level B and a very broad one considered as a base line, originating from the level A. Thus the height of Hanle curve (polarization in zero field) and its width are not attributable to A and therefore are independent of the height and the width of the Brossel curve. Comparison between these two curves was made on the 5994-Å line, where the three resonances due to the fine structure collapse into a single-resonance curve. The ratio of the heights of the two curves was measured for the 5994-Å line (Fig. 3), giving the value of $\frac{1}{3}$ which is in agreement with

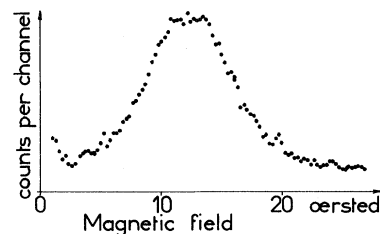


FIG. 3. Experimental resonance curve on the 5994-Å line at 21 MHz. This curve has been obtained from the experimental curve by subtracting the slightly curved base line. The centering of this curve required a correction of 0.5% because of the overlap with the symmetrical resonance at $-\omega$.

the ratio calculated for $b = 0.4$ in a direct process. This result confirms that the Hanle curve is due to the level under study.

In the second case, when the product $g\tau$ of the upper level is much smaller than that of level A , the observed Hanle effect is due to the level A , and the correspondence between the heights of individual Hanle and Brossel effects is unaffected by the cascade. Nevertheless, the relative heights (Sec. II) of the three fine structure contributions both in the Brossel and in the Hanle effects are no longer given by the calculations of Sec. II, Eqs. (4) and (7); in fact, coupling between \underline{N} and \underline{S} can occur in the upper level and the excitation matrix element ${}^J\rho^{(0)k}_q$ is no longer expressible as a function only of the term ${}^N\rho^{(0)k}_q$ (more detailed calculation have been made elsewhere^{33,34}). This situation is excluded in view of the agreement between the relative heights of the three resonances calculated (8) for the rotational level $N = 2$, and the experimental results on the 6230-Å line. It was necessary to exclude this possibility in order to permit the calculation of the three Hanle components in the $N = 2$ level. This calculation is crucial in order to obtain the value of τ and σ .

VI. CONCLUSION

The above experimental results permit us to con-

clude that for the $N = 1$ level the $\underline{N}\text{-}\underline{S}$ decoupling begins already at 21 MHz. Consequently, a natural extension of this study would be to perform further Brossel-type experiments at higher frequencies in order to determine the fine structure for this level (Paper II).²¹

The value of the g factors found at zero field leads us to believe that ${}^3\Pi_u$ corresponds to the pure Hund's case (b), as has already been pointed out by Dieke *et al.*³⁵ on the basis of his Zeeman experiments at high field (35 000 Oe). In this experiment where the electron spin was entirely decoupled from all other angular momenta, the observed g factor may be different from its zero-field value in the limit where the fine structure is larger than or of the order of $1/\tau$ (g factors being different for these two conditions). The interpretation of the Hanle results requires the knowledge of the zero-field g factor, which thus necessitates its determination at weak fields.

Finally, the experimentally determined values of τ and σ were found to be independent on N and v , to within the experimental error.

ACKNOWLEDGMENT

The authors are grateful to J. M. Castejon for the delicate work he has performed in constructing the glass triode cells.

¹D. R. Crosley and R. N. Zare, Phys. Rev. Letters **18**, 942 (1967); Bull. Am. Phys. Soc. **12**, 1147 (1967).

²M. A. Marechal, A. Jourdan, C. Nédélec, and J. C. Pebay-Peyroula, Compt. Rend. **268**, 1428 (1969).

³F. W. Dalby and J. Van der Linde, *Colloque A.M.P. E.R.E. XV* (North-Holland, Amsterdam, 1969); J. van der Linde, thesis (University of Vancouver, 1970) (unpublished).

⁴K. R. German and R. N. Zare, Phys. Rev. **186**, 9 (1969).

⁵A. Marshall, R. L. de Zafra, and H. Metcalf, Phys. Rev. Letters **22**, 445 (1969); Bull. Am. Phys. Soc. **14**, 620 (1969).

⁶M. McClintock, W. Demtröder, and R. N. Zare, J. Chem. Phys. **51**, 5509 (1969).

⁷S. J. Silvers, T. H. Bergeman, and M. Klemperer, J. Chem. Phys. **52**, 4385 (1970).

⁸R. C. Isler and W. C. Wells, Bull. Am. Phys. Soc. **14**, 622 (1969); W. C. Wells and R. C. Isler, Phys. Rev. Letters **24**, 705 (1970).

⁹R. W. Field and T. H. Bergeman, J. Chem. Phys. **54**, 2936 (1971).

¹⁰W. Hanle, Z. Physik **30**, 93 (1924).

¹¹M. A. Marechal and A. Jourdan, Phys. Letters **30A**, 31 (1969).

¹²K. German and R. N. Zare, Phys. Rev. Letters **23**, 1207 (1969).

¹³J. C. Lehmann, and G. Guedard, Compt. Rend. **270**, 1664 (1970).

¹⁴R. L. de Zafra, A. Marshall, and H. Metcalf, Phys. Rev. A **3**, 1557 (1971).

¹⁵J. Brossel and F. Bitter, Phys. Rev. **86**, 308 (1952).

¹⁶W. E. Lamb, Phys. Rev. **105**, 559 (1957).

¹⁷H. W. B. Skinner and E. T. S. Appleyard, Proc. Roy. Soc. (London) **117A**, 224 (1927).

¹⁸P. Cahill, R. Schwartz, and N. Jette, Phys. Rev. Letters **19**, 283 (1967).

¹⁹J. C. Pebay-Peyroula, J. Phys. Radium **20**, 669 (1959); **20**, 721 (1959).

²⁰M. Lombardi, J. Phys. Radium **30**, 631 (1969).

²¹R. Jost, M. A. Marechal, and M. Lombardi, following paper, Phys. Rev. A **5**, 740 (1972).

²²G. Herzberg, *Spectra of Diatomic Molecules* (Van Nostrand, Princeton, N. J., 1950).

²³M. I. D'Yakonov, Zh. Eksperim. i Teor. Fiz. **47**, 2213 (1964) [Sov. Phys. JETP **20**, 1484 (1965)]; Opt. i Spectroskopiya **19**, 662 (1965) [Opt. Spectry. **19**, 372 (1965)].

²⁴O. Nédélec, J. Phys. Radium **27**, 680 (1966); thèse (Grenoble, 1969) (unpublished).

²⁵J. C. Percival and M. J. Seaton, Phil. Trans. Roy. Soc. London **A251**, 113 (1958).

²⁶A. Omont and J. Meunier, Phys. Rev. **169**, 92 (1968).

²⁷A. Messiah, *Mécanique Quantique*, 2nd ed. (Dunod, Paris, 1964), p. 926.

²⁸J. P. Descoubes, Compt. Rend. **259**, 3733 (1964).

²⁹L. Y. Chow Chiu, Phys. Rev. **137**, A384 (1964).

³⁰W. Lichten, Phys. Rev. **120**, 8486 (1960).

³¹A. C. Mitchell and M. W. Zemansky, *Excited Atoms and Resonance Radiation* (Cambridge U.P., Cambridge, England, 1934).

³²M. Giroud, M. Lombardi, and J. C. Pebay-Peyroula, J. Phys. Radium **30**, 789 (1969).

³³M. Ducloy and M. Dumont, J. Phys. Radium **31**, 419

(1970).

³⁴M. Lombardi (unpublished).³⁵G. H. Dieke, S. P. Cunningham, and F. T. Byrne, Phys. Rev. 92, 81 (1953).

PHYSICAL REVIEW A

VOLUME 5, NUMBER 2

FEBRUARY 1972

Fine Structure of the $N = 1 (1s3p) {}^3\Pi_u$ State of the Hydrogen Molecule Determined by Magnetic Resonance

R. Jost, M. A. Marechal, and M. Lombardi

Université Scientifique et Médicale de Grenoble, Laboratoire de Spectrométrie Physique, CEDEX-53, Grenoble-Gare 38, France

(Received 28 July 1971)

In the preceding paper some of our results on the magnetic-resonance experiments performed at 64 MHz indicated a beginning of $\underline{N} \cdot \underline{S}$ decoupling on the $N = 1 (1s3p) {}^3\Pi_u$ state of H_2 excited by electron impact. In the present paper we present further results on the resonance experiments performed at higher frequencies in order to determine the fine structure of this level. Our findings indicate that the energy separation between $J = 1$ and $J = 2$ levels is 160 ± 5 MHz and between $J = 1$ and $J = 0$ levels it is 2100 ± 600 MHz, and in addition the former exhibits a small dependence on the vibrational number. The relative order of these levels is $J = 1, 2, 0$ instead of the theoretically predicted $2, 1, 0$. The Landé g factor is 1.249 ± 0.010 , which corresponds to a pure Hund's-coupling case (b).

I. INTRODUCTION

As was suggested in Paper I,¹ a study of the Bitter-Brossel resonance² as a function of frequency is performed on the optical transition ($\lambda = 5994 \text{ \AA}$) arising from the $(1s3p) {}^3\Pi_u$ ($v = 0, N = 1, S = 1, I = 0$) state of H_2 . This resonance, previously carried out at 21, 35, and 64 MHz, is extended to 105 and 147.6 MHz where the $\underline{N} \cdot \underline{S}$ decoupling is strong enough to separate the different resonances due to the Zeeman sublevels. The study of the position and the intensity of the resonances at 147.6 MHz enables us to deduce the following information about the fine structure of the level: the energy separation between the $J = 1$ and $J = 2$ levels, an order of magnitude of the energy of the $J = 0$ level, and the relative disposition of those three levels.

Similar work has been performed^{3, 4} on the $2 {}^3P$ and $3 {}^3P$ levels of He⁴. Our present theoretical treatment is similar to the one of Lamb,³ except for the intensity calculation. On the other hand, experimental conditions are more difficult than those of Ref. (4) (the lifetime τ of the studied level is three times shorter, the fine structure four times smaller, and the observed intensity is roughly 1000 times weaker in our case).

An extension of this experimental work at the next three vibrational (v) levels of the same electronic and rotational state enables us to estimate the dependence of the fine structure on v . We have also deduced from this study the Landé g factor of this state at zero magnetic field.

A level-crossing experiment at nonzero magnetic field⁵ may also be used to determine the magnitude of the fine structure. Such an experiment, current-

ly being performed in our laboratory has given preliminary results^{6, 7} which are in agreement with those reported here.

II. EXPERIMENTAL

The experimental setup for the excitation of H_2 and for the detection of the signal is the same as described in Paper I. At 105 MHz, as for 64 MHz,¹ the resolution of the resonances from the different Zeeman sublevels is not sufficiently good to justify precise measurements.

We present in Fig. 1 a resonance curve obtained at 147.6 MHz in the region of 60–180 Oe. We can see on this figure the continuous base line becoming increasingly curved with the magnetic field. The evaluation of the relative heights of the resonances depends on the determination of this base line. The shape of the base line which was found to be unchanged in the absence of rf field can be explained as follows: (i) a level anticrossing³ whose shape is the same as our base line; this effect exists even for constant excitation process, i. e., $Q_0 - Q_1 = \text{const}$ (see Appendix); (ii) a possible continuous change in the excitation process due to the modification of the electron trajectory by the static magnetic field which implies that $Q_0 - Q_1$ is a function of H_z ; (iii) a continuous change in the total emitted intensity with the magnetic field which can be as high as 30% and is only partially compensated by the detection system.⁸

The experimental resonance curves obtained at 35, 64, and 147.6 MHz are reproduced in Fig. 2, the base line being subtracted. The observations were repeated several times to verify the reproducibility of the measurements.